Modulational instability of electromagnetic waves in birefringent fibers with periodic and random dispersion

F. Kh. Abdullaev
Physical-Technical Institute of the Uzbek Academy of Sciences, G. Mavlyanov Street 2-b, 700084 Tashkent, Uzbekistan

J. Garnier*
Centre de Mathématiques Appliquées, Centre National de la Recherche Scientifique, Unité Mixte de Recherche 7641, Ecole Polytechnique, 91128 Palaiseau Cedex, France

(Received 24 February 1999)

Modulational instability (MI) of electromagnetic waves in a birefringent fiber with a periodic dispersion (two-step dispersion management scheme) is investigated. The properties of new sidebands are studied. The strong variation of dispersion leads to the decreasing of the main MI region and the suppression of additional resonance. In the random dispersion case the MI of all frequencies of modulation in the normal dispersion region is predicted. In the anomalous dispersion case the decreasing of the main MI peak is calculated and changes in the spectral bandwidth of MI gain are found. The analytical predictions are confirmed by the numerical simulations of the full coupled nonlinear Schrödinger equations with periodic coefficients. [S1063-651X(99)10907-3]

PACS number(s): 42.81.Gs, 42.65.−k, 42.50.Ar

I. INTRODUCTION

The modulational instability (MI) of nonlinear plane waves is one of the fundamental phenomena in the nonlinear waves physics. The history is about thirty years [1–5]. This phenomenon finds many applications in plasma physics, hydrodynamics, nonlinear optics, and other branches of physics. In particular, in nonlinear optics this phenomena is important for the optical communications systems (degradation of performance), the generation of short pulses with high repetition rates [5], and the design of all-optical logical devices [6].

The modulational instability phenomenon consists in the instability of nonlinear plane waves solutions against weak long scale modulations with frequencies lower than some critical value. The next stage of evolution is the growth of sidebands and the periodic exchange of energy between pump and sidebands due to the wave propagation. The scalar and vector nonlinear Schrödinger (NLS) equations have been studied in Refs. [7–10]. A lot of work has been devoted to the MI process in homogeneous nonlinear media.

Recently the investigation of the MI process in periodically modulated media has attracted attention [11–13]. This investigation is mainly motivated by the electromagnetic waves propagation in fibers with periodically varying power and dispersion along the propagation distance. The corresponding mathematical model is the NLS equation with periodically varying dispersion and nonlinear coefficients. A new phenomenon has been predicted: the generation of new sidebands and the existence of unstable sidebands even in the normal dispersion regime. The existence of such sidebands is connected with the parametric resonance between fiber parameters modulations and some characteristic frequencies. The periodic modulations of dispersion is of particular interest. As analysis shows, the periodic modulations of dispersion leads to decreasing of MI gain [14,15]. This result motivates the study of the dispersion-managed solitons [16,17].

It is interesting to investigate the extension of this problem to the vector NLS case. Physical motivations are MI in a birefringent fiber with periodic dispersion and gain. Recently the interest to this problem has increased due to polarization division multiplexing schemes in the dispersion-managed solitons applications. The numerical simulations of a birefringent fiber with the two-step dispersion managed scheme shows the existence of dispersion-managed solitons in this case [18]. MI with periodically modulated birefringence and periodically varying group velocity delay was analyzed recently by [19].

In this paper we shall also study the MI process in the case when the dispersion of the birefringent fiber is randomly modulated. In real fibers there always exist random fluctuations of parameters. The measurements of the longitudinal variations show that the zero wavelength λ_0 is fluctuating and this leads to the degradation of the optical communications system performance [20,21].

The paper is organized as follows. In Sec. II the model is described. The analysis of MI in the birefringent fiber with two-step dispersion managed scheme is performed in Sec. III. In Sec. IV the MI in the case of randomly modulated dispersion is studied and the MI gain and spectral behavior is calculated for the mean normal and anomalous dispersion cases.

II. DESCRIPTION OF THE MODEL

We shall study the propagation of two polarized electromagnetic waves in a periodic transmission line with an arbitrary dispersion $\beta(x)$. The governing system is the system of two coupled modified nonlinear Schrödinger equations [18]

*FAX: (33) 1 69 33 30 11. Electronic address: garnier@cmapx.polytechnique.fr

$$iu_x+\beta(x)u_{tt}+\gamma(|u|^2+\alpha|v|^2)u=0, \tag{1}$$

$$iv_x+\beta(x)v_{tt}+\gamma(\alpha|u|^2+|v|^2)v=0, \tag{2}$$

where x and t are conventionally normalized distance and time in the moving reference frame and $\alpha=1$ for orthogonally polarized waves. In the birefringent fiber case $\alpha\approx 2/3$. The dispersion coefficient $\beta(x)$ is a periodically x-varying function. The system has the nonlinear plane waves solutions

$$u_0=A\exp[i\gamma(A^2+\alpha B^2)x], \tag{3}$$

$$v_0=B\exp[i\gamma(B^2+\alpha A^2)x]. \tag{4}$$

Let us consider the modulational instability of those solutions. We perform a linear stability analysis, representing the solutions in the form

$$u=(A+u_1)e^{i\gamma(A^2+\alpha B^2)x}, \tag{5}$$

$$v=(B+v_1)e^{i\gamma(B^2+\alpha A^2)x}. \tag{6}$$

Then the equations for the corrections u_1, v_1 are

$$iu_{1x}+\beta(x)u_{1tt}+\gamma A^2(u_1+u_1^*)+\gamma\alpha AB(v_1+v_1^*)=0, \tag{7}$$

$$iv_{1x}+\beta(x)v_{1tt}+\gamma B^2(v_1+v_1^*)+\gamma\alpha AB(u_1+u_1^*)=0. \tag{8}$$

It is useful to perform the Fourier transform. We then get

$$iu_{1x}(\Omega)-\beta(x)\Omega^2u_1(\Omega)+\gamma A^2[u_1(\Omega)+u_1^*(-\Omega)]+\gamma\alpha AB[v_1(\Omega)+v_1^*(-\Omega)]=0, \tag{9}$$

$$iv_{1x}(\Omega)-\beta(x)\Omega^2v_1(\Omega)+\gamma B^2[v_1(\Omega)+v_1^*(-\Omega)]+\gamma\alpha AB[u_1(\Omega)+u_1^*(-\Omega)]=0. \tag{10}$$

Note that the system (7),(8) only contains second-order derivatives with respect to t, so that $u_1(t)=u_1(-t)$ and $v_1(t)=v_1(-t)$, which also imposes $u_1(\Omega)=u_1(-\Omega)$ and $v_1(\Omega)=v_1(-\Omega)$. We can then separate the system (9),(10) into the real and imaginary parts using $u_1=a+ib, v_1=c+id$. We get the system

$$a_x=\beta(x)\Omega^2b, \tag{11}$$

$$b_x=-\beta(x)\Omega^2a+2\gamma A(Aa+\alpha Bc), \tag{12}$$

$$c_x=\beta(x)\Omega^2d, \tag{13}$$

$$d_x=-\beta(x)\Omega^2c+2\gamma B(Bc+\alpha Aa). \tag{14}$$

Throughout the paper we shall consider the particular case $A=B$ which simplifies the algebra. Finally we shall define the MI gain as the coefficient $G(\Omega)$ which governs the maximal exponential growth of $a(\Omega)^2$, $b(\Omega)^2$, $c(\Omega)^2$, and $d(\Omega)^2$.

III. ANALYSIS FOR TWO-STEP DISPERSION MANAGED SCHEME

A. Expression of the MI gain

Let us consider now the particular configuration where β is stepwise constant and takes two different values β_1 and β_2 at regularly spaced intervals with lengths L_1 and L_2, respectively. The system is consequently periodic with period $L:=L_1+L_2$. More precisely

$$\beta(x)=\beta_1 \text{ if } x\in[nL,nL+L_1), \quad \text{for } n=0,1,\ldots,$$
$$=\beta_2 \text{ if } x\in[nL+L_1,(n+1)L), \quad \text{for } n=0,1,\ldots .$$

Equations (11)–(14) can be solved analytically over intervals where β is constant. Setting

$$f^{\pm}:=a\pm c,$$

$$g^{\pm}:=b\pm d,$$

the functions (f^+,g^+) and (f^-,g^-) satisfy closed-form and independent equations. Over intervals of type j (where $\beta=\beta_j$), $j=1$ or 2, (f^+,g^+) and (f^-,g^-) satisfy

$$f^{\pm}_{xx}+\beta_j\Omega^2(\beta_j\Omega^2-l^{\pm-1})f^{\pm}=0,$$

$$g^{\pm}=f^{\pm}_x/(\beta_j\Omega^2),$$

where l^+ and l^- are the characteristic wavelengths

$$l^{\pm}:=\frac{1}{2\gamma A^2(1\pm\alpha)}. \tag{15}$$

Applying continuity conditions of the field and of its time derivative at the boundaries, it is then obvious to compute the general solutions of these linear differential equations with constant coefficients

$$\begin{pmatrix} f^{\pm} \\ g^{\pm} \end{pmatrix}(nL+L_1)=M_1^{\pm}(L_1)\begin{pmatrix} f^{\pm} \\ g^{\pm} \end{pmatrix}(nL),$$

$$\begin{pmatrix} f^{\pm} \\ g^{\pm} \end{pmatrix}[(n+1)L]=M_2^{\pm}(L_2)\begin{pmatrix} f^{\pm} \\ g^{\pm} \end{pmatrix}(nL+L_1),$$

where the matrices $M_j^{\pm}$ are given by

$$M_j^{\pm}(x)=\begin{pmatrix} \cos(k_j^{\pm}x) & \dfrac{\beta_j\Omega^2}{k_j^{\pm}}\sin(k_j^{\pm}x) \\ -\dfrac{k_j^{\pm}}{\beta_j\Omega^2}\sin(k_j^{\pm}x) & \cos(k_j^{\pm}x) \end{pmatrix}, \tag{16}$$

with

$$k_j^{\pm}(\Omega):=\sqrt{\beta_j\Omega^2(\beta_j\Omega^2-l^{\pm-1})}. \tag{17}$$

Note that if the expression inside the squared root is negative valued, then $k_j^{\pm}$ is imaginary, and the cos and sin which appear in Eq. (16) should then be interpreted as cosh and i sinh. Denoting

$$M^{\pm} := M_2^{\pm}(L_2) M_1^{\pm}(L_1)$$

we get the recursive relation

$$\begin{pmatrix} f^{\pm} \\ g^{\pm} \end{pmatrix}[(n+1)L] = M^{\pm} \begin{pmatrix} f^{\pm} \\ g^{\pm} \end{pmatrix}(nL),$$

from which we deduce that

$$\begin{pmatrix} f^{\pm} \\ g^{\pm} \end{pmatrix}(nL) = M^{\pm n} \begin{pmatrix} f^{\pm} \\ g^{\pm} \end{pmatrix}(0).$$

More generally, if $x \in [nL, nL+L_1)$, then

$$\begin{pmatrix} f^{\pm} \\ g^{\pm} \end{pmatrix}(x) = M_1^{\pm}(x-nL) M^{\pm n} \begin{pmatrix} f^{\pm} \\ g^{\pm} \end{pmatrix}(0)$$

and if $x \in [nL+L_1, (n+1)L)$, then

$$\begin{pmatrix} f^{\pm} \\ g^{\pm} \end{pmatrix}(x) = M_2^{\pm}(x-nL-L_1) M_1^{\pm}(L_1) M^{\pm n} \begin{pmatrix} f^{\pm} \\ g^{\pm} \end{pmatrix}(0).$$

We shall observe an exponential growth of a, b, c, or d (or equivalently f^+, g^+, f^-, or g^-) if and only if one of the eigenvalues of M^+ and M^- has a modulus larger than 1. Let us denote the two eigenvalues of M^+ (M^-) by λ_1^+ and λ_2^+ (λ_1^- and λ_2^-). Since $\det M^{\pm} = 1$, we have

$$\lambda_1^{\pm} \lambda_2^{\pm} = 1, \tag{18}$$

so that there is stability only when $|\lambda_1^+| = |\lambda_2^+| = |\lambda_1^-| = |\lambda_2^-| = 1$. Otherwise, there is MI gain and the exponential gain per unit length is given by

$$G = \frac{2}{L} \max(\ln|\lambda_1^+|, \ln|\lambda_2^+|, \ln|\lambda_1^-|, \ln|\lambda_2^-|).$$

From Eq. (18), this expression can be simplified into

$$G = \frac{2}{L} \max(|\ln|\lambda_1^+||, |\ln|\lambda_1^-||).$$

Let us now study more carefully the spectra of the matrices $M^{\pm}$. One finds that the eigenvalues have the following forms:

$$\lambda_1^{\pm} = a^{\pm} + \sqrt{a^{\pm 2} - 1},$$

$$\lambda_2^{\pm} = a^{\pm} - \sqrt{a^{\pm 2} - 1},$$

where

$$a^{\pm} := \cos(k_2^{\pm} L_2)\cos(k_1^{\pm} L_1) - \frac{1}{2}(r^{\pm} + r^{\pm -1}) \times \sin(k_2^{\pm} L_2)\sin(k_1^{\pm} L_1), \tag{19}$$

$$r^{\pm} := \frac{k_1^{\pm} \beta_2}{k_2^{\pm} \beta_1}. \tag{20}$$

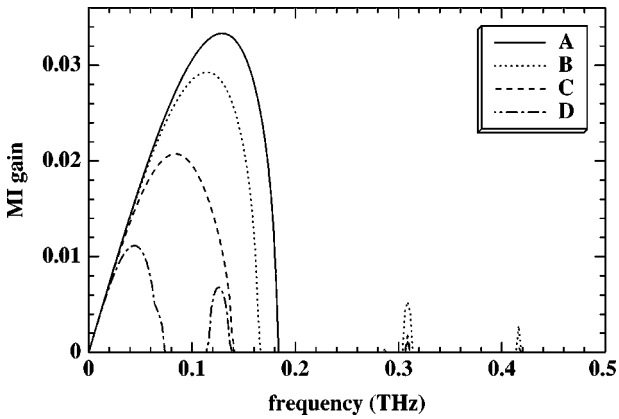

FIG. 1. MI gain per unit length (in km) versus modulation frequency Ω (in THz) for $\gamma = 2$ $W^{-1}\,km^{-1}$, $L_1 = L_2 = 20$ km, $P_0 = A^2 = 5$ mW, and $\alpha = 2/3$. The curve A corresponds to the standard anomalous dispersion $\beta_1 = \beta_2 = 1$ $ps^2\,km^{-1}$. Curves B, C, and D have all the same average anomalous dispersion $(L_1\beta_1 + L_2\beta_2)/(L_1 + L_2) = 1$ $ps^2\,km^{-1}$, but the dispersion management gets large values; B corresponds to $\beta_1 = 4$ and $\beta_2 = -2$ $ps^2\,km^{-1}$, C corresponds to $\beta_1 = 8$ and $\beta_2 = -6$ $ps^2\,km^{-1}$, and D corresponds to $\beta_1 = 16$ and $\beta_2 = -14$ $ps^2\,km^{-1}$.

Note that $a^{\pm}$ is always real valued even when $k_1^{\pm}$ and/or $k_2^{\pm}$ is complex valued. This can be checked by simple algebra using the fact that $k_j^{\pm}$ is either real valued or purely imaginary.

Two cases are possible.

(i) If $a^{\pm 2} > 1$, then the eigenvalues $\lambda_1^{\pm}$ and $\lambda_2^{\pm}$ are real valued and strictly different. Since the product $\lambda_1^{\pm}\lambda_2^{\pm}$ is equal to 1, at least one of the eigenvalues has a modulus larger than 1.

(ii) If $a^{\pm 2} \leqslant 1$, then, denoting $b^{\pm} := \sqrt{1 - a^{\pm 2}}$, the eigenvalues are given by $\lambda_1^{\pm} = a^{\pm} + ib^{\pm}$ and $\lambda_2^{\pm} = a^{\pm} - ib^{\pm}$. Since their product is equal to 1, we have $a^{\pm 2} + b^{\pm 2} = 1$, which means that there exists some $\theta^{\pm}$ such that $a^{\pm} = \cos(\theta^{\pm})$ and $b^{\pm} = \sin(\theta^{\pm})$. Consequently, $\lambda_1^{\pm} = \exp i\theta^{\pm}$ and $\lambda_2^{\pm} = \exp -i\theta^{\pm}$ have both modulus 1.

As a conclusion, there is stability if and only if $a^{-2} - 1$ and $a^{+2} - 1$ are nonpositive valued, and otherwise the exponential gain is

$$G = \frac{2}{L} \max(|\ln||a^+| + \sqrt{a^{+2} - 1}||, |\ln||a^-| + \sqrt{a^{-2} - 1}||). \tag{21}$$

$a^{\pm}$ depends on all parameters of the problem, namely, β_1, β_2, L_1, L_2, α, and A, and also on the frequency Ω through $k_j^{\pm}$ defined by Eq. (17). Equation (21) reads as a closed-form expression which allows us to plot $G(\Omega)$ as a function of Ω given the set of parameters $(\beta_1, \beta_2, L_1, L_2, \alpha, A)$.

B. Numerical applications

Figure 1 corresponds to the case of birefringent fibers with an average anomalous dispersion, when $\alpha = 2/3$. We have considered the case when $\gamma = 2$ $W^{-1}km^{-1}$, $L_1 = L_2 = 20$ km, $P_0 = A^2 = 5$ mW. In such conditions the characteristic wavelengths are $l^+ = 30$ km and $l^- = 150$ km. It appears

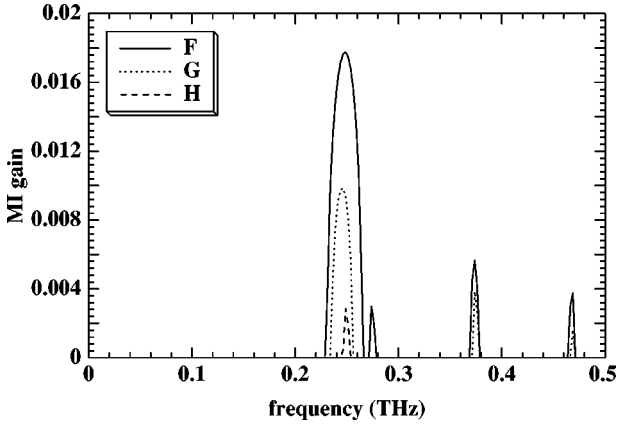

FIG. 2. MI gain per unit length (in km) versus modulation frequency Ω (in THz) for $\gamma=2\ \mathrm{W}^{-1}\,\mathrm{km}^{-1}$, $L_1=L_2=20$ km, $P_0=A^2=5$ mW, and $\alpha=2/3$. Curves *F*, *G*, and *H* have all the same average normal dispersion $(L_1\beta_1+L_2\beta_2)/(L_1+L_2)=-1\ \mathrm{ps}^2\,\mathrm{km}^{-1}$, but the dispersion management gets large values; *F* corresponds to $\beta_1=-3$ and $\beta_2=1\ \mathrm{ps}^2\,\mathrm{km}^{-1}$, *G* corresponds to $\beta_1=-4$ and $\beta_2=2\ \mathrm{ps}^2\,\mathrm{km}^{-1}$, and *H* corresponds to $\beta_1=-8$ and $\beta_2=6\ \mathrm{ps}^2\,\mathrm{km}^{-1}$.

that the central peak gain is progressively reduced as the strength of the dispersion management increases, and so are the resonant sidebands. We shall give more detail in the next section.

Figure 2 corresponds to the case of birefringent fibers with an average normal dispersion, when $\alpha=2/3$. Although there is no MI gain in the uniform case $\beta\equiv-1$ [9], some new sidebands appear when the dispersion management is not zero, but these sidebands tend to disappear for strong dispersion management.

C. Study of the case $L_1,\ L_2\ll l^+,\ l^-$

Let us study the MI gain in the framework when L_1 and L_2 are smaller than the characteristic wavelengths l^+ and l^-, which is usually the case in experimental configurations. We then introduce the adimensional parameter s such that $L_1=(1-s)L$ and $L_2=sL$. In such conditions the average dispersion is

$$\overline{\beta}:=(1-s)\beta_1+s\beta_2. \tag{22}$$

Here are the main results. The primary effect of dispersion management in the average anomalous dispersion case $(\overline{\beta}>0)$ is to reduce the central peak. When there is no dispersion management (i.e., $\beta\equiv\overline{\beta}>0$), the cutoff frequency of the central peak is

$$\Omega_+^2:=1/(\overline{\beta}l^+). \tag{23}$$

Substituting the ansatz $\hat{\Omega}_+=\Omega_+[1+b_1(L/l^+)+b_2(L/l^+)^2]$ into the expression (19) of $a^+(\Omega)$ and computing the expansion of $a^+(\hat{\Omega}_+)$ with respect to L/l^+, one finds that the central peak stands for frequencies Ω below a new cutoff frequency $\hat{\Omega}_+$ smaller than Ω_+:

$$\hat{\Omega}_+^2=\Omega_+^2\left[1-\frac{1}{12}\frac{(\beta_1-\beta_2)^2}{\overline{\beta}^2}s^2(1-s)^2\frac{L^2}{l^{+2}}+O\left(\frac{L^3}{l^{+3}}\right)\right]. \tag{24}$$

Furthermore, we can also compute the expansion of the MI gain inside this frequency band:

$$G(\Omega)=2\overline{\beta}\Omega\sqrt{\Omega_+^2-\Omega^2}\left[1-\frac{1}{24}\frac{(\beta_1-\beta_2)^2\Omega^2}{\overline{\beta}^2(\Omega_+^2-\Omega^2)}s^2(1-s)^2\times\frac{L^2}{l^{+2}}+O\left(\frac{L^3}{l^{+3}}\right)\right]. \tag{25}$$

It then clearly appears that a strong dispersion management reduces the central peak. Furthermore, if the averaged dispersion $\overline{\beta}$ and the period L is fixed, the reduction is all the more important as $|\beta_1-\beta_2|$ is large and $s=1/2$, which corresponds to the case $L_1=L_2$. Moreover we can compare the formula (24) with the exact plot of the MI gain given in Fig. 1. It appears that Eq. (24) is very accurate for the configurations A, B, and C, but not for the configuration D. Indeed the dispersion management in case D is so large that further terms in the expansion (24) should be taken into account.

We can also give more information about the resonant peaks. They appear in the vicinities of some particular frequencies Ω_p, $p=1,2,3,\ldots$, which can be expanded as powers of L:

$$\Omega_p^2=\frac{1}{L}(c_{1,p}+c_{2,p}L+c_{3,p}L^2+\cdots).$$

Substituting this ansatz into the expression (19) of a^+ and collecting the terms with the same power of L one can identify the first coefficients of the expansion $c_{1,p}$ and $c_{2,p}$. It is found that the coefficient $c_{1,p}$ depend only on $|\overline{\beta}|$. It means in particular that the resonances appear equivalently for an anomalous or a normal average dispersion. For each p, there are two suitable corrective terms $c_{2,p}$ that we denote by $c_{2,p}^+$ and $c_{2,p}^-$ since they correspond to l^+ and l^-, respectively. We shall see that the peak corresponding to l^+ is much higher.

$$c_{1,p}=\frac{p\pi}{|\overline{\beta}|},$$

$$c_{2,p}^{\pm}=\frac{1}{2\overline{\beta}l^{\pm}},$$

so that the resonant frequencies are

$$\Omega_p^{\pm 2}=\frac{p\pi}{|\overline{\beta}|L}+\frac{1}{2\overline{\beta}l^{\pm}}. \tag{26}$$

Let us apply the formula (26) to the configuration corresponding to Fig. 1. One finds that the theoretical resonant peaks should be around $\Omega_1^+\sim0.31$, $\Omega_1^-\sim0.29$, $\Omega_2^+\sim0.42$, $\Omega_2^-\sim0.40$, $\Omega_3^+\sim0.50$, and $\Omega_3^-\sim0.49$ (in THz). The comparison with the exact plot of the MI gain given in Fig. 1 is therefore excellent. The same holds true for the

comparison with Fig. 2, when the theoretical resonant peaks are predicted to be around $\Omega_1^+ \sim 0.25$, $\Omega_1^- \sim 0.275$, $\Omega_2^+ \sim 0.375$, $\Omega_2^- \sim 0.39$, $\Omega_3^+ \sim 0.47$, and $\Omega_3^- \sim 0.48$ (in THz).

The positions of the resonant frequencies do not depend on the strength dispersion management $\beta_1 - \beta_2$, but the maxima of the corresponding peaks do. We now focus on this point. Let us consider a frequency around $\Omega_p^{\pm}$ and expand the expression (19) of $a^{\pm}$. The corresponding expansion of the MI gain G defined as Eq. (21) is

$$G(\sqrt{\Omega_p^{\pm 2}+\Omega^2}) = \sqrt{[1-(-1)^p \cos\theta_p]\frac{(\beta_2-\beta_1)^2\overline{\beta^2}}{2\beta_1^2\beta_2^2\pi^2 p^2 l^{\pm 2}} - 4\overline{\beta^2}\Omega^4} + O\left(\frac{L}{l^{\pm}}\right), \tag{27}$$

$$\theta_p := \frac{\beta_1(1-s)-\beta_2 s}{\beta_1(1-s)+\beta_2 s} p\pi. \tag{28}$$

The MI gain peak is reached in $\Omega_p^{\pm}$ and is equal to $[1-(-1)^p \cos\theta_p]^{1/2}|\beta_2-\beta_1|\overline{\beta}/(\sqrt{2}|\beta_1||\beta_2| l^{\pm}\pi p)$. But it may happen that $\cos\theta_p$ is equal to $(-1)^p$. In such a case the term inside the square root in the right hand side of Eq. (27) is always nonpositive, so that one has to determine the next term [in $O(L/l^{\pm})$] in the expansion of G. If $\cos\theta_p = (-1)^p$, then the MI gain in the vicinity of the resonant frequency $\Omega_p^{\pm}$ is given by

$$G\left(\sqrt{\Omega_p^{\pm 2}+\Omega^2\frac{L}{l^+}}\right) = \sqrt{\frac{1}{4}\left(\frac{\tilde{\beta}^{-1}\overline{\beta}-1}{\pi p l^{\pm}}\right)^2 - 4\left(\overline{\beta}\Omega^2 - \frac{\tilde{\beta}^{-1}\overline{\beta}}{8\pi p l^{\pm}}\right)^2}\frac{L}{l^{\pm}} + O\left(\frac{L^2}{l^{\pm 2}}\right), \tag{29}$$

$$\tilde{\beta}^{-1} := (1-s)\beta_1^{-1} + s\beta_2^{-1}. \tag{30}$$

The MI gain peak is reached in $\sqrt{\Omega^{\pm 2} + L/(\tilde{\beta} 8\pi p l^{\pm 2})}$ and is equal to $|\overline{\beta}\tilde{\beta}^{-1}-1|L/(2\pi p l^{\pm 2})$. Note that this peak can be canceled only if $s=0$, $s=1$, or $\beta_1=\beta_2$, i.e., when the dispersion management is zero. Furthermore when the dispersion management increases, the maximum of the peak goes to its minimal value $L/(2\pi p l^{\pm 2})$.

Figure 3 plots the MI gain in the vicinities of the two first resonant peaks for some particular configurations. Let us first consider the peaks corresponding to Ω_1^+ [Fig. 3(a)]. In the configurations *I*, *K*, and *M*, we have $\theta_1 = 2\pi$, $\theta_1 = 4\pi$, and $\theta_1 = 6\pi$, respectively. Accordingly we apply formula (27) which shows that the resonant peaks are rather important. In the configurations *J* and *L*, we have $\theta_1 = 3\pi$ and $\theta_1 = 5\pi$ respectively. Accordingly we apply formula (29) which shows that the corresponding peaks are rather low. Let us now consider the peak corresponding to Ω_2^+ [Fig. 3(b)]. In all configurations the normalized angle θ_2/π is an even number. Application of formula (29) then yields that the corresponding peaks are low and similar.

D. Numerical simulations of the modulational instability

In this section we perform detailed comparison of predictions of the above theory with a full numerical investigation of the problem. We use the split-step algorithm to solve the vector NLS equations (1),(2). As an initial condition we choose

$$u_0(x) = A[1+\sigma m(x)],$$

$$v_0(x) = A,$$

where $m(x)$ is white noise with a flat spectrum and $\sigma \ll 1$. The system then naturally amplifies the frequencies which correspond to the MI gain spectrum, and computing the spectrum of the transmitted wave we directly get the sum of a Dirac peak centered at $\Omega = 0$ (corresponding to the unperturbed problem $u_0 = A$, $v_0 = A$) and of the spectrum of the MI gain.

In Fig. 4 we investigate the same configuration as in Fig. 1 (average anomalous dispersion). We choose $\sigma = 5\times 10^{-6}$ and make the wave propagate over a distance 400 km. The picture is in very good agreement with the theoretical one.

In Fig. 5 we investigate the same configuration as in Fig. 2 (average normal dispersion). We choose $\sigma = 5\times 10^{-6}$ and make the wave propagate over a distance 800 km. In the standard normal dispersion (i.e., $\beta \equiv -1$) we can observe an almost flat spectrum which means that there is no MI gain. Furthermore dispersion management creates resonances at the frequencies derived in the above theoretical model, but as the strength of dispersion management is increased, these resonant peaks are progressively suppressed.

IV. RANDOM MODULATIONS OF DISPERSION

A. Formulation of the problem

In this section we study the influence of random modulations of dispersion on MI in a birefringent fiber. The dispersion is represented as $\beta(x) = \beta_0 + \beta_1(x)$. The fluctuations of the dispersion are assumed to obey Gaussian statistics with correlation function

$$\langle \beta_1(x)\beta_1(y)\rangle = B(x-y;l_c), \tag{31}$$

where l_c is the correlation length. When $l_c \to 0$, we have the white noise case $B(x-y;l_c) \to 2\sigma^2\delta(x-y)$. We adopt the same notations as in the above sections. The system of equations for $f^{\pm}, g^{\pm}$ is

$$f_x^{\pm} = \beta(x)\Omega^2 g^{\pm}, \tag{32}$$

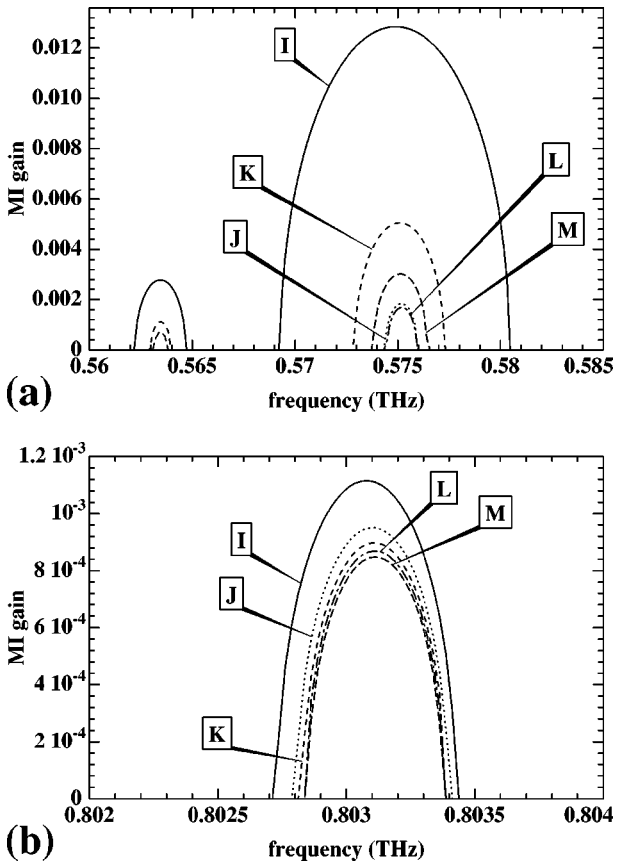

FIG. 3. MI gain per unit length (in km) versus modulation frequency Ω (in THz) for $\gamma=2\ \mathrm{W}^{-1}\,\mathrm{km}^{-1}$, $L_1=L_2=5$ km, $P_0=A^2=5$ mW, and $\alpha=2/3$. (a) [(b)] is focused around the first resonant peak Ω_1^+ (the second resonant peak Ω_2^+). In (a) the peak corresponding to Ω_1^- is also noticeable. The curves have all the same average anomalous dispersion $\overline{\beta}=1\ \mathrm{ps}^2\,\mathrm{km}^{-1}$, but the dispersion management gets large values; *I* corresponds to $\beta_1=3$ and $\beta_2=-1\ \mathrm{ps}^2\,\mathrm{km}^{-1}$, *J* corresponds to $\beta_1=4$ and $\beta_2=-2\ \mathrm{ps}^2\,\mathrm{km}^{-1}$, *K* corresponds to $\beta_1=5$ and $\beta_2=-3\ \mathrm{ps}^2\,\mathrm{km}^{-1}$, *L* corresponds to $\beta_1=6$ and $\beta_2=-4\ \mathrm{ps}^2\,\mathrm{km}^{-1}$, and *M* corresponds to $\beta_1=7$ and $\beta_2=-5\ \mathrm{ps}^2\,\mathrm{km}^{-1}$.

$$g_x^{\pm}=-\beta(x)\Omega^2 f^{\pm}+2\gamma A^2(1\pm\alpha)f^{\pm}. \tag{33}$$

The analysis of the system of equations for the first moments $\langle f^{\pm}\rangle,\langle g^{\pm}\rangle$ shows that the dynamics is the exponential decreasing of first moments and that the resonant phenomena are absent. This is an expected phenomenon, since $f^{\pm}$ and $g^{\pm}$ are strongly oscillating and these oscillations make the first moments average to 0. So we shall analyze the behaviors of the second moments $\langle f^{\pm 2}\rangle$, $\langle g^{\pm 2}\rangle$, and $\langle f^{\pm}g^{\pm}\rangle$ (we add $\langle f^{\pm}g^{\pm}\rangle$ so as to close the equations for the second moments). The system of equations for the second order moments has the form:

$$\langle f^{\pm 2}\rangle_x=2\beta_0\Omega^2\langle f^{\pm}g^{\pm}\rangle+2\Omega^2\langle\beta_1(x)f^{\pm}g^{\pm}\rangle, \tag{34}$$

$$\langle g^{\pm 2}\rangle_x=2(l^{\pm -1}-\beta_0\Omega^2)\langle f^{\pm}g^{\pm}\rangle-2\Omega^2\langle\beta_1(x)f^{\pm}g^{\pm}\rangle, \tag{35}$$

$$\langle f^{\pm}g^{\pm}\rangle_x=\beta_0\Omega^2\langle g^{\pm 2}\rangle+(l^{\pm -1}-\beta_0\Omega^2)\langle f^{\pm 2}\rangle+\Omega^2\langle\beta_1(x)(g^{\pm 2}-f^{\pm 2})\rangle. \tag{36}$$

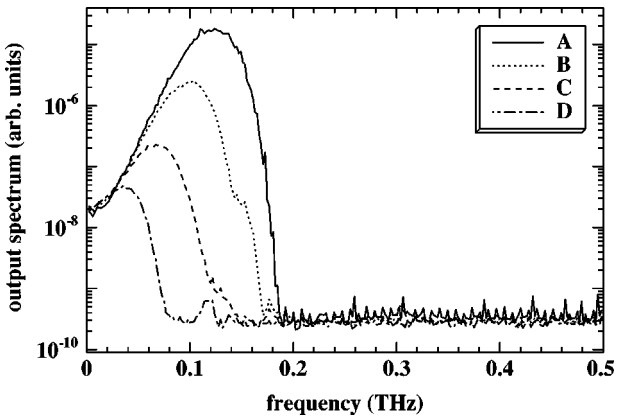

FIG. 4. Output spectrum after a propagation over 400 km of the initial wave (u_0,v_0) for $\gamma=2\ \mathrm{W}^{-1}\,\mathrm{km}^{-1}$, $L_1=L_2=20$ km, $P_0=A^2=5$ mW, $\sigma=10^{-5}$, and $\alpha=2/3$. Curve *A* corresponds to the standard anomalous dispersion $\beta_1=\beta_2=1\ \mathrm{ps}^2\,\mathrm{km}^{-1}$. Curves *B*, *C*, and *D* have all the same average anomalous dispersion $(L_1\beta_1+L_2\beta_2)/(L_1+L_2)=1\ \mathrm{ps}^2\,\mathrm{km}^{-1}$, but the dispersion management gets large values; *B* corresponds to $\beta_1=4$ and $\beta_2=-2\ \mathrm{ps}^2\,\mathrm{km}^{-1}$, *C* corresponds to $\beta_1=8$ and $\beta_2=-6\ \mathrm{ps}^2\,\mathrm{km}^{-1}$, and *D* corresponds to $\beta_1=16$ and $\beta_2=-14\ \mathrm{ps}^2\,\mathrm{km}^{-1}$.

where l^+ and l^- are defined by Eq. (15). For decoupling of the means $\langle\beta_1 f^{\pm}g^{\pm}\rangle,\langle\beta_1 f^{\pm 2}\rangle,\langle\beta_1 g^{\pm 2}\rangle$ we apply the Furutzu-Novikov formulas

$$\langle\beta_1(x)F\rangle=\int_0^x dy\,B(x-y)\left\langle\frac{\delta F(x)}{\delta\beta_1(y)}\right\rangle. \tag{37}$$

As a result we obtain the system for the second moments which reads as a linear system

$$\frac{d}{dx}\begin{pmatrix}\langle f^{\pm 2}\rangle\\ \langle g^{\pm 2}\rangle\\ \langle f^{\pm}g^{\pm}\rangle\end{pmatrix}=M^{\pm}\begin{pmatrix}\langle f^{\pm 2}\rangle\\ \langle g^{\pm 2}\rangle\\ \langle f^{\pm}g^{\pm}\rangle\end{pmatrix}, \tag{38}$$

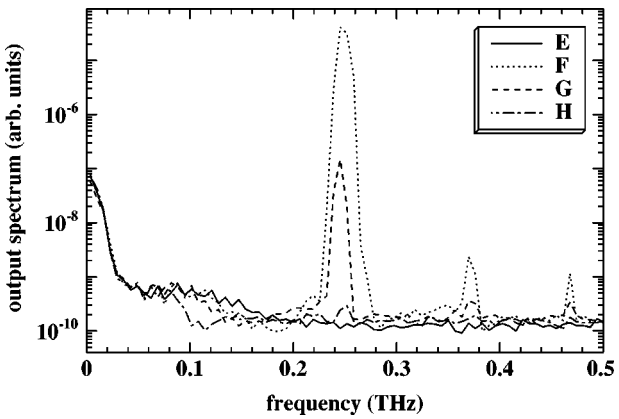

FIG. 5. Output spectrum after a propagation over 800 km of the initial wave (u_0,v_0) for $\gamma=2\ \mathrm{W}^{-1}\,\mathrm{km}^{-1}$, $L_1=L_2=20$ km, $P_0=A^2=5$ mW, $\sigma=10^{-5}$, and $\alpha=2/3$. Curve *E* corresponds to the standard normal dispersion $\beta_1=\beta_2=1\ \mathrm{ps}^2\,\mathrm{km}^{-1}$. Curves *E*, *F*, and *G* have all the same average normal dispersion $(L_1\beta_1+L_2\beta_2)/(L_1+L_2)=1\ \mathrm{ps}^2\,\mathrm{km}^{-1}$, but the dispersion management gets large values; *F* corresponds to $\beta_1=-3$ and $\beta_2=1\ \mathrm{ps}^2\,\mathrm{km}^{-1}$, *G* corresponds to $\beta_1=-4$ and $\beta_2=2\ \mathrm{ps}^2\,\mathrm{km}^{-1}$, and *H* corresponds to $\beta_1=-8$ and $\beta_2=6\ \mathrm{ps}^2\,\mathrm{km}^{-1}$.

$$M^{\pm}=\begin{pmatrix} -2\Omega^4\sigma^2 & 2\Omega^4\sigma^2 & 2\beta_0\Omega^2 \\ 2\Omega^4\sigma^2 & -2\Omega^4\sigma^2 & 2(l^{\pm -1}-\beta_0\Omega^2) \\ (l^{\pm -1}-\beta_0\Omega^2) & \beta_0\Omega^2 & -4\Omega^4\sigma^2 \end{pmatrix}. \tag{39}$$

Instability is actually present if an eigenvalue of M^+ or M^- has a positive real part, and the MI gain, which corresponds to an exponential growth of $\langle f^{\pm 2}\rangle$ or $\langle g^{\pm 2}\rangle$, is the largest value of the real parts of the eigenvalues of $M^{\pm}$. We have found that the matrices M^+ and M^- have three eigenvalues denoted by (p_1^+,p_2^+,p_3^+) and (p_1^-,p_2^-,p_3^-), respectively. These eigenvalues can be expanded as powers of σ^2:

$$p_1^{\pm}=2\Omega\sqrt{\beta_0(l^{\pm -1}-\beta_0\Omega^2)} + \frac{1}{2}\frac{\Omega^2(8\beta_0^2\Omega^4-8\beta_0\Omega^2 l^{\pm -1}+l^{\pm -2})}{\beta_0(l^{\pm -1}-\beta_0\Omega^2)}\sigma^2+O(\sigma^4), \tag{40}$$

$$p_2^{\pm}=-2\Omega\sqrt{\beta_0(l^{\pm -1}-\beta_0\Omega^2)} + \frac{1}{2}\frac{\Omega^2(8\beta_0^2\Omega^4-8\beta_0\Omega^2 l^{\pm -1}+l^{\pm -2})}{\beta_0(l^{\pm -1}-\beta_0\Omega^2)}\sigma^2+O(\sigma^4), \tag{41}$$

$$p_3^{\pm}=-\frac{\Omega^2 l^{\pm -2}}{\beta_0(l^{\pm -1}-\beta_0\Omega^2)}\sigma^2+O(\sigma^4). \tag{42}$$

B. Normal dispersion $\beta_0<0$

In this case, the real parts of $p_1^{\pm}$ and $p_2^{\pm}$ are negative, and $p_3^{\pm}$ is positive real valued for every frequency Ω, which proves that there is instability for all frequencies. The gain is equal to p_3^+ (because $l^+<l^-$ implies $p_3^+>p_3^-$):

$$G(\Omega)=\frac{\Omega^2 l^{+-2}}{|\beta_0|(l^{+-1}+|\beta_0|\Omega^2)}\sigma^2+O(\sigma^4).$$

The MI peak corresponds to $\Omega\to\infty$ and is given by

$$G^{\mathrm{opt}}=\frac{1}{\beta_0^2 l^{+2}}\sigma^2+O(\sigma^4)=\frac{4\gamma^2A^4(1+\alpha)^2}{\beta_0^2}\sigma^2+O(\sigma^4).$$

C. Anomalous dispersion $\beta_0>0$

We introduce the characteristic frequencies $\Omega_{\pm}$, $\Omega_{1,\pm}$, and $\Omega_{2,\pm}$:

$$\Omega_{\pm}^2:=\frac{1}{\beta_0 l^{\pm}}, \tag{43}$$

$$\Omega_{1,\pm}^2:=\frac{2-\sqrt{2}}{4}\Omega_{\pm}^2, \tag{44}$$

$$\Omega_{2,\pm}^2:=\frac{2+\sqrt{2}}{4}\Omega_{\pm}^2. \tag{45}$$

We can then rewrite $p_1^{\pm}$, $p_2^{\pm}$, and $p_3^{\pm}$ as follows:

$$p_1^{\pm}=2\beta_0\Omega\sqrt{\Omega_{\pm}^2-\Omega^2}+4\frac{\Omega^2(\Omega^2-\Omega_{1,\pm}^2)(\Omega^2-\Omega_{2,\pm}^2)}{\Omega_{\pm}^2-\Omega^2}\sigma^2 + O(\sigma^4), \tag{46}$$

$$p_2^{\pm}=-2\beta_0\Omega\sqrt{\Omega_{\pm}^2-\Omega^2}+4\frac{\Omega^2(\Omega^2-\Omega_{1,\pm}^2)(\Omega^2-\Omega_{2,\pm}^2)}{\Omega_{+}^2-\Omega^2}\sigma^2 + O(\sigma^4), \tag{47}$$

$$p_3^{\pm}=\frac{\Omega^2\Omega_{\pm}^4}{\Omega^2-\Omega_{\pm}^2}\sigma^2+O(\sigma^4). \tag{48}$$

In the standard MI region $\Omega<\Omega_+$, the gain is now given by p_1^+:

$$G(\Omega)=2\beta_0\Omega\sqrt{\Omega_+^2-\Omega^2}+4\frac{\Omega^2(\Omega^2-\Omega_{1,+}^2)(\Omega^2-\Omega_{2,+}^2)}{\Omega_+^2-\Omega^2}\sigma^2 + O(\sigma^4),$$

which shows that the random dispersion makes instability increase for $\Omega\in(0,\Omega_{1,+})$ and $\Omega\in(\Omega_{2,+},\Omega_+)$, and decrease for $\Omega\in(\Omega_{1,+},\Omega_{2,+})$. In particular, the MI peak which is obtained around $\Omega=\Omega_+/\sqrt{2}$ is reduced:

$$G^{\mathrm{opt}}=\beta_0\Omega_+^2-\frac{1}{2}\Omega_+^4\sigma^2+O(\sigma^4).$$

In the standard stable region $\Omega>\Omega_+$, the gain is now positive for every frequency and of order σ^2, since the dominant terms in $p_1^{\pm}$ and $p_2^{\pm}$ are imaginary. Comparing carefully the real parts of $p_1^{\pm}$, $p_2^{\pm}$, and $p_3^{\pm}$ then establishes that the gain is imposed by p_3^+:

$$G(\Omega)=\frac{\Omega^2\Omega_+^4}{\Omega^2-\Omega_+^2}\sigma^2+O(\sigma^4).$$

D. Numerical applications

The above analysis of normal and anomalous dispersion was performed under the assumption that the fluctuations were weak in the sense that $\sigma\ll|\beta_0|$. This is usually the case in standard applications, but we can actually compute the eigenvalues of the matrix M for any σ. They are the roots of a polynomial of degree 3, so that the Cartan rule [22] gives closed form expressions for the roots which are complicated, but can be plotted easily.

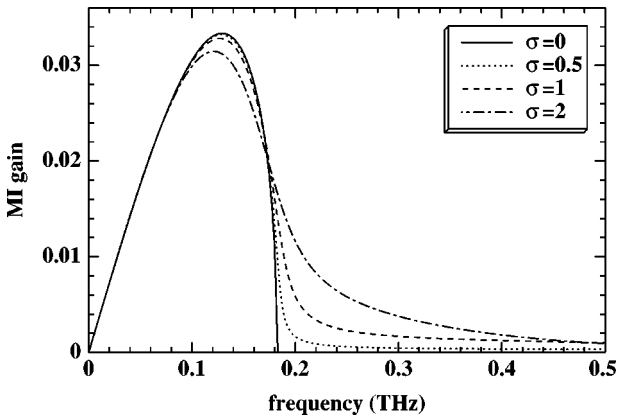

FIG. 6. MI gain per unit length (in km) versus modulation frequency Ω (in THz) for $\gamma=2\ \mathrm{W}^{-1}\,\mathrm{km}^{-1}$, $L_1=L_2=20$ km, $P_0=A^2=5$ mW, and $\alpha=2/3$. The solid curve corresponds to the standard anomalous dispersion $\beta_0=1\ \mathrm{ps}^2\,\mathrm{km}^{-1}$ and $\sigma=0$. The dashed curves have all the same average anomalous dispersion $\beta_0=1\ \mathrm{ps}^2\,\mathrm{km}^{-1}$, but the standard deviations σ (expressed in $\mathrm{ps}^2\,\mathrm{km}^{-1}$) of the fluctuations of the dispersion have different values.

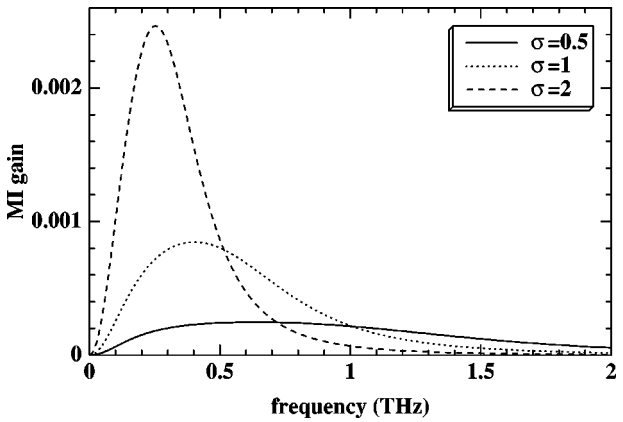

FIG. 7. MI gain per unit length (in km) versus modulation frequency Ω (in THz) for $\gamma=2\ \mathrm{W}^{-1}\,\mathrm{km}^{-1}$, $P_0=A^2=5$ mW, and $\alpha=2/3$. The curves have all the same average normal dispersion $\beta_0=-1\ \mathrm{ps}^2\,\mathrm{km}^{-1}$, but the standard deviations σ (expressed in $\mathrm{ps}^2\,\mathrm{km}^{-1}$) of the fluctuations of the dispersion have different values.

We first consider a case where the average dispersion is anomalous. As shown by Fig. 6 the central peak remains almost unchanged even when the standard deviation of the fluctuations of the dispersion is equal to the average dispersion β_0. The standard deviation of the fluctuations has to be larger than β_0 to involve a noticeable departure of the central peak from its unperturbed form corresponding to $\sigma=0$. The main effect of the fluctuations is in fact to make the frequencies just above the cutoff frequency Ω_+ very unstable.

Let us now regard a case where the average dispersion is normal. If there is no instability in the unperturbed normal dispersion case, we can check in Fig. 7 that the fluctuations of the dispersion make all frequencies all the more unstable as the fluctuations are larger.

V. CONCLUSION

In conclusion we have investigated the modulational instabilities of electromagnetic waves in birefringent fibers with periodic dispersion (two-step dispersion management scheme). We have found that the strong periodic modulation of dispersion leads to the suppression of resonant sidebands and essentially reduces the spectral width of the main peak of MI. These results can be important for the dispersion management optical communication using vector optical solitons.

The modulational instability of nonlinear plane waves in the birefringent fibers with random dispersion has been analyzed. We have found that in the normal dispersion region all frequencies are modulationally unstable (in the deterministic case we have not MI). The gain in this region is $\sim A^4\sigma^2/\beta_0^2$. In the anomalous dispersion case the behavior of MI is more complicated. In the region of frequencies of modulations $0<\Omega<\Omega_{1,+}$ and $\Omega_{2,+}<\Omega<\Omega_+$ the gain is enhanced and in the region $\Omega_{1,+}<\Omega<\Omega_{2,+}$ (where the optimal frequency lies) the gain is reduced by comparison with the deterministic case. In the stable region for deterministic case ($\Omega>\Omega_+$) the inclusion of random dispersion leads to instabilities for all frequencies of modulations.

As a final remark we would like to point out that it would be also interesting to consider the MI in fibers with random group velocity delay and random linear birefringence. These problems will be investigated separately.

ACKNOWLEDGMENT

F. Kh. Abdullaev acknowledges partial support from INTAS (Grant No. 96-0339).

[1] A. A. Vedenov and L. I. Rudakov, Dokl. Akad. Nauk SSSR **159**, 767 (1964) [Sov. Phys. Dokl. **9**, 1073 (1965)].
[2] V. I. Bespalov and V. I. Talanov, JETP Lett. **3**, 307 (1966).
[3] L. A. Ostrowski, Zh. Éksp. Teor. Fiz. **51** 1189 (1966) [Sov. Phys. JETP **24**, 797 (1967)].
[4] T. B. Benjamin and J. E. Feir, J. Fluid Mech. **27**, 417 (1967).
[5] K. Tai, A. Hasegawa, and A. Tomita, Phys. Rev. Lett. **21**, 209 (1968).
[6] M. Islam, *Ultrafast all Optical Devices* (Oxford University Press, Oxford, 1992).
[7] A. I. Berkhoer and V. E. Zakharov, Zh. Éksp. Teor. Fiz. **58**, 903 (1970) [Sov. Phys. JETP **31**, 486 (1970)].
[8] G. P. Agrawal, Phys. Rev. Lett. **59**, 880 (1987).
[9] J. E. Rothenberg, Phys. Rev. Lett. **64**, 813 (1987).
[10] S. Wabnitz, Phys. Rev. A **38**, 2018 (1988).
[11] F. Matera, A. Meccozzi, M. Romagnoli, and M. Settembre, Opt. Lett. **18**, 1499 (1993).
[12] F. Kh. Abdullaev, JETP **20**, 25 (1994).
[13] F. Kh. Abdullaev, S. A. Darmanyan, S. Bishoff, and M.P. Sørensen, J. Opt. Soc. Am. B **14**, 27 (1997).
[14] N. J. Smith and N. J. Doran, Opt. Lett. **21**, 570 (1996).
[15] J. Bronski and N. Kutz, Opt. Lett. **21**, 937 (1996).

[16] N. J. Smith, F. M. Knox, N. J. Doran, K. J. Blow, and I. Bennion, Electron. Lett. **32**, 54 (1996).
[17] I. Gabitov and S. K. Turitsyn, Opt. Lett. **21**, 327 (1997).
[18] T. Georges, J. Opt. Soc. Am. B **15**, 1553 (1998).
[19] S. G. Murdoch, M. D. Thomson, R. Leonhardt, and J. D. Harvey, Opt. Lett. **22**, 682 (1997).
[20] F. Kh. Abdullaev, S. A. Darmanyan, A. Kobyakov, and F. Lederer, Phys. Lett. A **220**, 213 (1996).
[21] M. Karlsson, J. Opt. Soc. Am. B **15**, 2269 (1998).
[22] M. Abramowitz and I. Stegun, *Handbook of Mathematical Functions* (Dover, New York, 1965).